

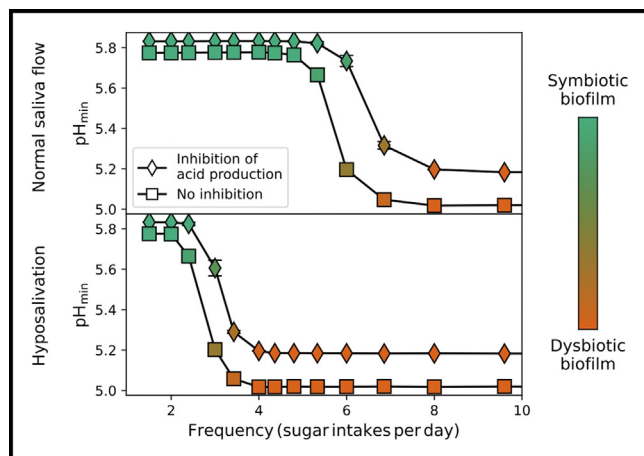
ORIGINAL RESEARCH

In silico study of hyposalivation and sugar exposure on biofilm dysbiosis



David Head, PhD^a; Philip D. Marsh, PhD^b; Deirde Devine, PhD^b;
Livia M. A. Tenuta, DDS, MS, PhD^c

^aSchool of Computing, University of Leeds, Leeds, United Kingdom; ^bDivision of Oral Biology, School of Dentistry, University of Leeds, St James University Hospital, Leeds, United Kingdom; ^cDepartment of Cariology, Restorative Sciences, and Endodontics, School of Dentistry, University of Michigan, Ann Arbor, MI.



Why Is This Important?

Caries is caused by a microbial biofilm (dental plaque) that readily metabolizes dietary sugars into harmful acids, gradually forming a caries lesion. As the biofilm becomes more acidic, there is a selection of bacterial species that better survive in this environment and are more cariogenic, a process called dysbiosis. A high frequency of sugar intake per day drives the dental biofilm into a dysbiotic state faster. Patients with reduced saliva production (hyposalivation) are particularly susceptible to dysbiosis because of the lessened rate of acid removal from the tooth surfaces by salivary flow and reduced buffering of generated acids; under such conditions, the authors estimated using computer modeling that the biofilm turns dysbiotic even under a low frequency of sugar intake per day. In this study, the authors used this mathematical model to systematically determine which factors (sugar intake frequency, inhibitors of bacterial acid production) could prevent dysbiosis under hyposalivation. Although interventions to reduce acidity alone can theoretically be effective, current inhibitors would be incapable of preventing dysbiosis. The authors conclude that the only effective means to maintain a symbiotic biofilm in hyposalivation is to limit the frequency of fermentable sugar intake episodes stringently.

© 2022 The Author(s). Published by Elsevier Inc. on behalf of the American Dental Association. This is an open access article under the CC BY-NC-ND license (<http://creativecommons.org/licenses/by-nc-nd/4.0/>).
<https://doi.org/10.1016/j.jfscie.2022.100019>

Abstract

Background. Dental caries develops under actively sugar-fermenting dental biofilms, but the most successful control methods available only target mineral loss. Reduced salivary flow rates (hyposalivation) significantly exacerbate caries progression by lessening sugar and acid clearance near tooth surfaces. Maintaining dental biofilm symbiosis (health) under hyposalivation requires knowledge of the impact of acid inhibition under given dietary regimens.

Methods. An individual-based mathematical model was used to predict biofilm dysbiosis under normal or hyposalivatory conditions by regulating the frequency of sugar intake and inhibiting microbial glycolysis, reducing the acid challenge to the tooth mineral. The impact of pH-dependent (stronger inhibition at lower pH [eg, fluoride]) and pH-independent (general percentage reduction in acid production) strategies on pH near the tooth surface during sugar intake, and the corresponding compositional changes in the biofilm, were quantified.

Results. Under normal saliva flow, reducing the frequency of sugar intake and increasing the inhibition of acid production by pH-dependent or pH-independent strategies could prevent bacterial dysbiosis and prevent the biofilm from having a caries-associated (dysbiotic) to a health-

(Continued on next page)

associated (symbiotic) composition. However, under hyposalivatory conditions, dysbiosis occurred beyond 2 sugar intakes per day, and the degree of inhibition of glycolysis required to prevent dysbiosis was not feasible with available therapeutics.

Conclusions. Model data predict that to counteract the drastic effect of hyposalivation on biofilm dysbiosis, it will be essential to significantly reduce the frequency of fermentable sugar intake and any direct inhibition of bacterial metabolism.

Key Words. Caries; mathematical modeling; plaque biofilms; microbial ecology; saliva.

Introduction

The mouth harbors a diverse and complex collection of microorganisms—the oral microbiome—that delivers essential benefits to their host.¹ However, this mutually beneficial relationship with the host, termed symbiosis, can break down because of alterations in the oral environment, such as a change in diet or a reduced flow of saliva. These changes can drive shifts in the composition of the microbiome in which previously minor components of the biofilm become more competitive and eventually more numerous, leading to disease.

Caries is an example of a disease resulting from dental biofilm dysbiosis. Defined as a ubiquitous (bacteria + diet)-driven disease,² the interactions between bacteria and dietary sugars, leading to the production of acids and the selection of acid-tolerating (and acidogenic) species in the biofilm, are central to the caries process. In patients affected by hyposalivation, the biofilm is particularly susceptible to change, and much lower frequencies of sugar intake are predicted to lead to biofilm dysbiosis and an increased risk of caries.³ Although fluoride can reduce caries rates in these patients, its effect is mainly restricted to the balance of mineral loss or gain.⁴ Caries control in these challenging conditions could be improved if additional approaches are applied that significantly reduce sugar metabolism and thereby prevent biofilm dysbiosis.

Previously, the concept of control without killing^{5,6} has been explored, in which inhibitors that affect biofilm metabolism could lead to long-term effects on the disease process by reducing the growth and activity of acidogenic microorganisms without necessarily killing them, thereby favoring the maintenance of a symbiotic biofilm. Several different inhibitors of microbial metabolism (tin, zinc, fluoride), compounds that raise local pH (arginine, urea), or non-metabolizable sugar substitutes would fall into this category of agents that could reduce the ecological pressure for biofilm dysbiosis caused by acid produced under a high daily frequency of sugar exposure. Therefore, we sought to investigate if the inhibition of acid production in the dental biofilm could counteract the deleterious effect of sugar on biofilm dysbiosis under hyposalivation or whether dietary control should be the prime target for dental professionals.

Using an *in silico* model used to investigate the effect of hyposalivation on biofilm dysbiosis,³ here we explore the effects of varying sugar frequency and inhibiting microbial acid production by defined incremental amounts, under normal and reduced saliva flow conditions, on biofilm dysbiosis.

Methods

Experimental design

Biofilms comprising nonaciduric and aciduric bacterial species were modeled using computer simulations similar to those previously described^{3,7} but with modifications highlighted below. Parameters were varied in each simulation of biofilm dysbiosis to explore the effect of an inhibition of acid production and a reduction in the frequency of sugar intake under conditions of normal salivary flow or hyposalivation.

Because of the crucial effect of biofilm pH on biofilm dysbiosis⁸ and variations in the mechanism of action of inhibitors known to affect bacterial metabolism (eg, fluoride is an inhibitor of bacterial acid production but is mainly effective at lower pH values⁹), 2 types of inhibition of biofilm metabolism were tested: pH-dependent, in which inhibition was 50% at pH^{50%} and increased as the pH decreased (acidity increased), or pH-independent, in which inhibition was a percentage *Indep%* irrespective of environmental pH.

In silico model overview

The 3-dimensional geometry describing the biofilm-rich region close to the tooth surface and the distant saliva layer is given in [Figure 1A](#). Biomass (bacteria + matrix) aggregates were represented as spheres, and dispersed sugar and acid phases as smoothly varying concentration fields.¹⁰ Nutrient (sugar) was introduced by imposing a predefined glucose concentration (*[G]*) at the saliva-air interface. Although sucrose is the dietary sugar most relevant to caries, difficulties introduced by glucan production have resulted in the relatively limited characterization of the kinetics of metabolism compared with glucose, which has been extensively characterized *in vitro*. We, therefore, followed Head et al.⁷ and used published data for glucose to parameterize bacterial metabolism, but allowance was made in the model to recognize the enhanced matrix production from sucrose. Long-time biofilm evolution has been shown to be only weakly sensitive to the rate of matrix production.¹¹

The salivary flow was modeled by a variable rate of sugar clearance from the biofilm environment, as used in early saliva flow models¹² and subsequently confirmed *in vitro* to be the primary effect with regard to caries.¹³ For normal

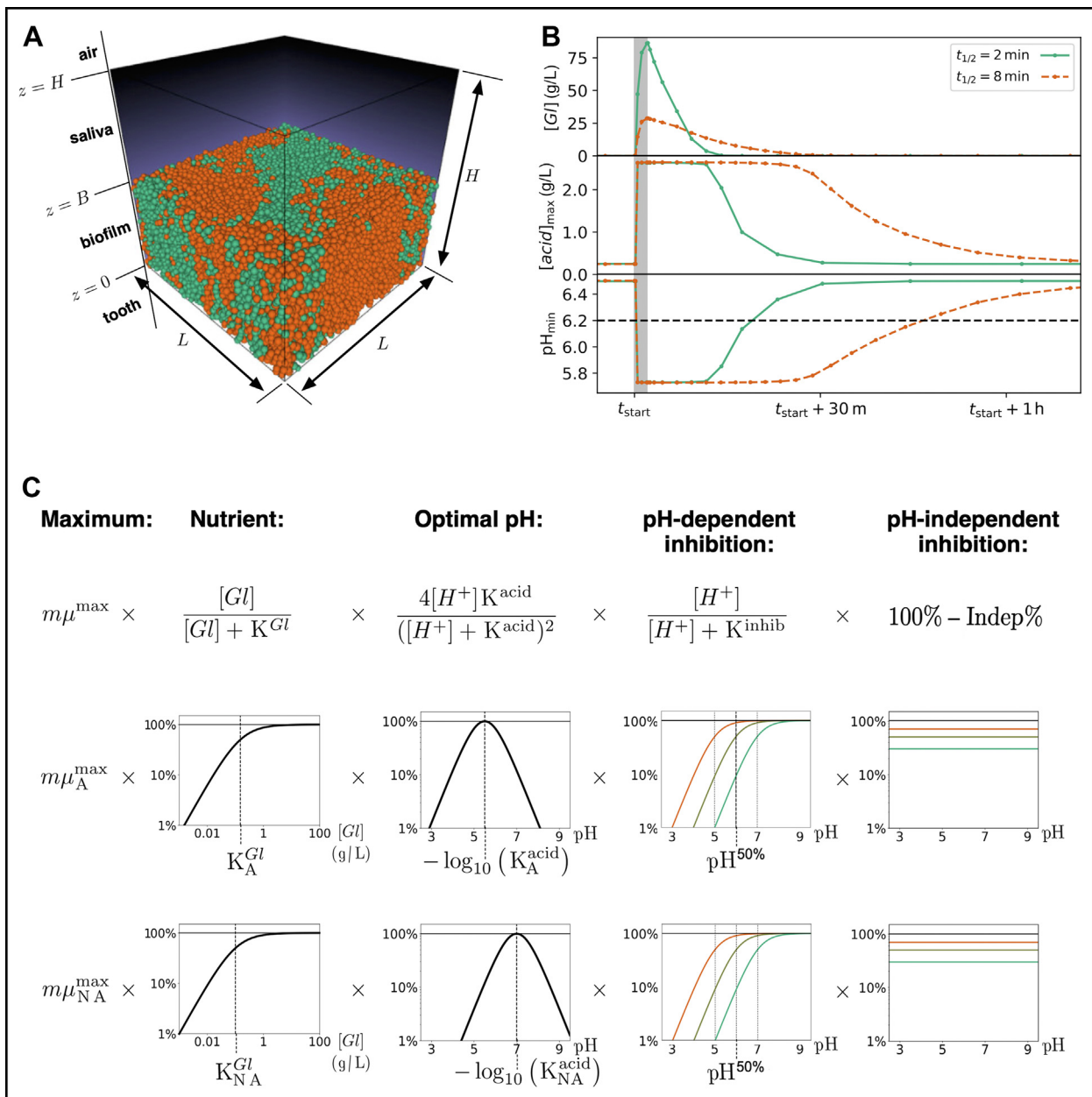


Figure 1 Diagrammatic representation of key model components. **A.** Simulation box annotated with the biofilm thickness B and the distance H between the tooth surface and saliva-air interface. Particles of type A and NA are shown as spheres with different colors. **B.** Single sugar pulse in a symbiotic biofilm under normal ($t_{1/2} = 2$ min) and hyposalivatory ($t_{1/2} = 8$ min) conditions, showing resultant predissociated acidity and postdissociated pH at the tooth surface. **C.** The glycolytic rate for a particle of mass m as a function of local glucose concentration $[Gl]$ and pH, showing the general equation (top row) and graphical representations of each factor for particles of type A (middle row) and NA (lower row). Separate lines are shown for pH-dependent inhibition $pH^{50\%}$ equals $-\log_{10}(K_{inhib}^{50\%})$ equals 5, 6, and 7, and pH-independent inhibition $\text{Indep}\%$ equals 30%, 50% and 70%.

conditions, $[Gl]$ quickly peaked and decayed with a half-life of $t_{1/2}$ equals 2 minutes, following the detailed single-pulse modeling of Ilie et al.^{14,15} In vivo observations suggest a 4-fold increase in clearance times for hyposalivation,¹⁶ so a much slower decay of $t_{1/2}$ equals 8 minutes was used for this condition. The integrated area under the curve (total available glucose) was the same for both conditions, so peak concentration was higher under normal conditions (Figure 1B).

These fixed pulses were repeated at regular intervals representing episodes of dietary intake.

Biomass metabolism

The biomass was described by 2 particle types representing functional groupings of bacteria with opposing contributions to biofilm cariogenicity.¹⁷ Particles labeled A, for aciduric

(acid tolerant) bacteria, could metabolize environmental sugars to acid even at low pH, comparable to species associated with supragingival biofilm dysbiosis in caries. The second particle type, labeled NA for nonaciduric (non-acid-tolerant bacteria), could not significantly metabolize sugars at low pH, relating to species associated with symbiosis and dental health.

The conversion of carbohydrate $[Gl]$ to acid $[acid]$ for a particle of type A and mass m occurred at a rate

$$r = m \mu_A^{max} \times \frac{[Gl]}{[Gl] + K_A^{Gl}} \times \frac{4[H^+]K_A^{acid}}{([H^+] + K_A^{acid})^2} \times \frac{[H^+]}{[H^+] + K^{inhib}} \times (100\% - \text{Indep}\%),$$

with a similar expression for NA. As graphically displayed in Figure 1C, the factors on the right-hand side correspond to (in order) the maximum rate, nutrient uptake with limitation, preferred acidity, pH-dependent inhibition, and pH-independent inhibition, respectively. $K_{A,NA}^{Gl}$ and $K_{A,NA}^{acid}$ were intrinsic parameters inferred from a range of in vitro characterization experiments as detailed in Head et al.,⁷ and we used the same parameters in this related model (as in other models,^{3,11,15} in vivo experiments can be used to inform model phenomenology but are generally unsuitable for parameterizing bacterial metabolism). $[H^+]$ was the acidity after dissociation, found from the concentration $[acid]$ before dissociation using an empirical buffering curve.¹⁸ The pH-dependent factor described inhibition in the form of a reduced glycolytic rate when $[H^+]$ was similar to or less than K^{inhib} , with K^{inhib} assumed to be the same for A and NA. For convenience, K^{inhib} is replaced below by the corresponding pH at which the inhibition is exactly 50%, $pH^{50\%}$ equals $-\log_{10}(K^{inhib})$. Inhibition independent of acidity was implemented by uniformly lowering the reaction rate by the same percentage, $\text{Indep}\%$, for both A and NA.

Two additional reactions were included. The nutrient supply $[Gl]$ was augmented by exogenous and endogenous carbohydrates present in the biofilm matrix and the saliva, $[polyGl]$,¹⁹ which obeyed the same glycolysis equation as $[Gl]$, but at a much lower concentration than the peak value of $[Gl]$, and was constant in space and time. Particles could also be killed (removed from the system) because of high acidity, modeled as a death rate $10^7 K^{death}[H^+]$, with K_{NA}^{death} equals $2K_A^{death}$ equals $4 \times 10^{-3}/h$.

Biomass growth

Cellular growth was proportional to the rate of acid production r by a relative yield Y_A or Y_{NA} (ie, particles of mass m grew at a rate $\frac{dm}{dt}$ equals $Y_{A,NA}r$, with an additional factor for matrix production). Particles were divided into 2 daughters of the same type whenever a threshold aggregate radius was reached, in which, for simplicity, the same threshold was chosen for both types, r_A^{max} equals r_{NA}^{max} equals 6.25 μm .

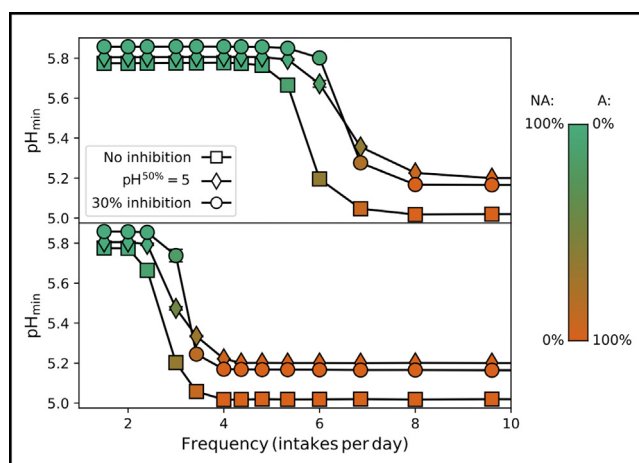


Figure 2 The predicted effect of frequency of sugar intake on biofilm composition and the pH generated at the tooth surface during a sugar challenge. The upper panel corresponds to normal salivary flow conditions $t_{1/2}$ equals 2 minutes, and the lower panel corresponds to hyposalivatory conditions $t_{1/2}$ equals 8 minutes. For each, separate curves are shown for no inhibition, pH-dependent inhibition $pH^{50\%}$ equals 5, and pH-independent inhibition $\text{Indep}\%$ equals 30%. Symbols are colored according to the composition of the biofilm after 50 days, as per the calibration bar to the right, where A denotes aciduric particles and NA denotes nonaciduric particles.

Constant biofilm thickness was maintained by removing particles with centers $z > B$ equals 250 μm , similar to the constant-depth film fermenter.²⁰

Results

Hyposalivation promotes dysbiotic biofilms

During each glucose pulse, the acid generated from glycolysis lowered the environmental pH, further enhancing the acid production of the aciduric A particles relative to NA particles. Because metabolism was directly linked to growth in the model, this resulted in a concomitant increase in the number of A particles throughout a single sugar pulse. Conversely, the neutral pH of biofilms between pulses favored the growth of NA particles. Therefore, the net effect over many pulses was expected to depend on sugar intake frequency, with high frequencies continuously shifting the biofilm composition toward dysbiosis (ie, dominated by particles of type A), as observed in earlier modeling studies.^{7,11} Figure 2 confirmed this trend, which also shows the minimum pH at the tooth surface was lower for dysbiotic biofilms than for symbiotic (NA-dominated) ones, justifying our use of these terms.

The trends for rapid sugar removal under normal conditions were also observed for hyposalivatory conditions with retarded sugar removal. The primary difference was the lower critical intake frequency for the crossover to dysbiosis to become apparent under hyposalivation (Figure 2), leading to the prediction of dysbiosis for some dietary regimes that would still promote symbiotic biofilms under normal salivary

flow conditions. There was no measurable change in the minimum pH during a pulse in either the symbiotic or dysbiotic biofilms. This is consistent with model assumptions: hyposalivation was assumed to alter the profile of the sugar pulse by extending its duration with a reduced peak value, integrating the same total sugar availability per pulse. However, as shown by the Stephan curves²¹ in Figure 1B, even this reduced peak was sufficient to saturate glycolysis for both particle types. The effect of the slow sugar removal under hyposalivation was to increase the duration of acid challenges rather than to modulate peak acidity.

Inhibition of acid production promotes symbiotic biofilms but cannot counteract the effect of hyposalivation

Both types of inhibition of acid production we tested, pH-dependent inhibition (controlled by varying the parameter $\text{pH}^{50\%}$, defined such that the degree of inhibition was 50% at pH equals $\text{pH}^{50\%}$ and stronger for greater acidity) and pH-independent inhibition (assessed by lowering the rate of acid production, for all particles and for all times, by a fixed inhibition percentage $\text{Indep}\%$) (Figure 1C) resulted in (1) increased critical sugar intake frequency necessary to promote dysbiosis and (2) reduced peak acidity for all biofilm compositions (Figure 2). Both observations are consistent with reduced growth of A particles relative to NA particles because of the less acidic environment modulated by the inhibition. Data in Figure 2 also suggested some quantitative differences between the 2 forms of inhibition. Nevertheless, as highlighted by the distinct differences between normal salivary flow and hyposalivation seen in Figure 2, pH-dependent or pH-independent inhibition was insufficient to markedly change the frequency of sugar intake that can cause dysbiosis under hyposalivation.

The combinations of intake frequency and pH-dependent inhibition that predicted dysbiotic biofilms are given in Figure 3A and B for normal and hyposalivatory conditions, respectively. The broad dysbiotic region for the hyposalivatory data allowed the orientation of the boundary between symbiosis and dysbiosis to be unambiguously discerned and the sensitivity of the biofilm composition to inhibition to be inferred. The symbiotic-dysbiotic boundary is approximately vertical for weak inhibition $\text{pH}^{50\%}$ of 5 or less (labeled I in Figure 3B). The transition to dysbiosis occurred at a sugar intake frequency of around 3 times per day, irrespective of the strength of inhibition, indicating biofilm composition is only weakly responsive to acid inhibition. This highlights that inhibition alone has limited efficacy against a diet with a high frequency of fermentable carbohydrates under hyposalivatory conditions. The data also emphasize the critical importance of fermentable sugar intake frequency on dysbiosis under conditions of hyposalivation; merely exceeding just 2 intakes per day was sufficient to drive the biofilm to a dysbiotic state.

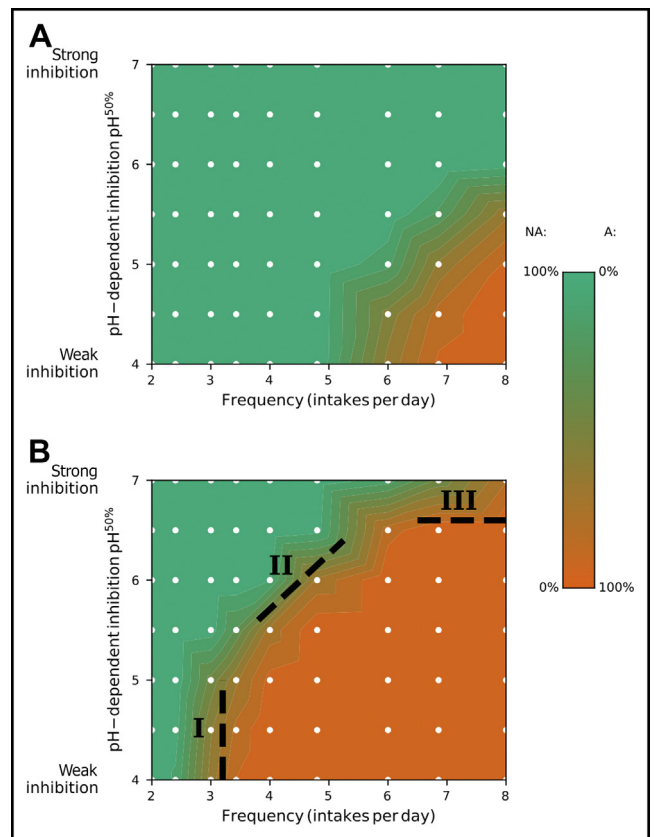


Figure 3 Contour plots showing the variation in biofilm composition as the degree of pH-dependent inhibition $\text{pH}^{50\%}$ and the sugar intake frequency were simultaneously varied. Separate plots are given for normal salivary flow (A) and hyposalivatory conditions (B). The regions marked I, II, and III in B are discussed in the text. The calibration bar to the right gives the biofilm composition after 50 days, where A denotes aciduric particles and NA denotes nonaciduric particles. White disks denote actual data points, with regions between points filled by linear interpolation.

The symbiotic-dysbiotic boundary approaches horizontally for high sugar intake frequencies (labeled III in Figure 3B). This indicates that the transition to dysbiosis in this region happens around the same inhibition, $\text{pH}^{50\%}$ of approximately 6.5, irrespective of the frequency of sugar intake. Thus, in this region of the parameter space, and in contrast to region I, the transition to dysbiosis is now highly sensitive to inhibition, and at most weakly responsive to sugar intake frequency. In between these 2 extremes, the symbiotic-dysbiotic boundary exhibits an intermediate slope (denoted by II in the Figure 3B), in which varying sugar intake frequency or inhibition could select between symbiotic or dysbiotic biofilms, and neither contribution was dominant.

Figure 4 shows the results for inhibition extending pH-independent inhibition from 0% through nearly full inhibition at 90% for both normal and hyposalivatory conditions. As in the case of pH-dependent inhibition, the primary effect of pH-independent inhibition was to promote symbiotic biofilms, requiring stronger inhibition in situations with

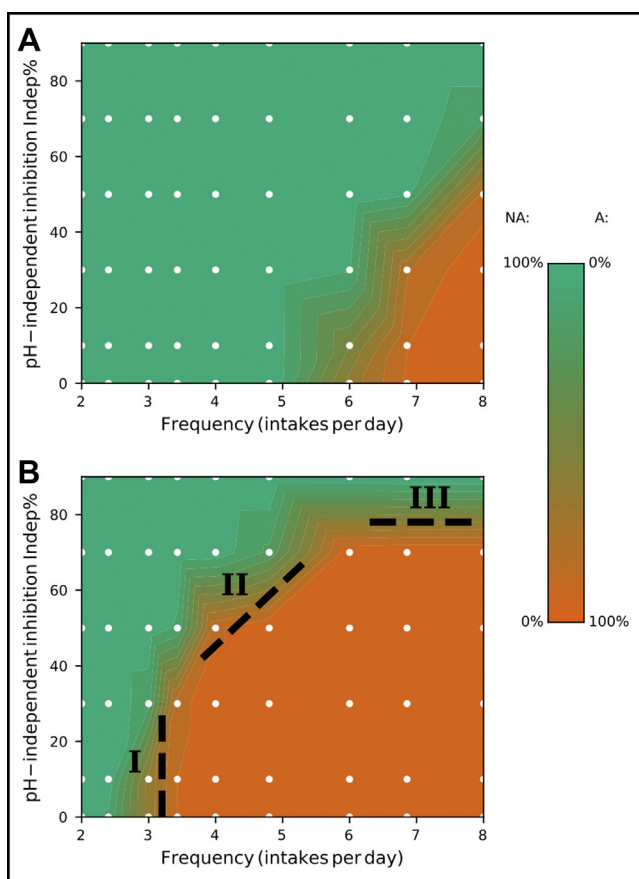


Figure 4 Contour plots show the variation in biofilm composition as the degree of pH-independent inhibition and the sugar intake frequency were simultaneously varied. Separate plots are given for normal salivary flow (**A**) and hyposalivatory conditions (**B**). The regions marked I, II, and III in **B** are discussed in the text. The calibration bar to the right gives the biofilm composition after 50 days, where A denotes aciduric particles and NA denotes non-aciduric particles. White disks denote actual data points, with regions between points filled by linear interpolation.

more frequent sugar intake. As before, the dysbiotic region was broader for hyposalivatory conditions than normal ones. For hyposalivation, the boundary between symbiotic and dysbiotic biofilms could again be delineated into regions corresponding to low sensitivity to inhibition (region I in [Figure 4B](#)), high sensitivity (region III), and an intermediate region in which both inhibition and intake frequency made comparable contributions to biofilm composition (region II). These broad similarities suggest that pH-independent inhibition has a similar overall effect on maintaining biofilm symbiosis as pH-dependent inhibition. However, the degree of inhibition required to prevent dysbiosis needs to be high.

Discussion

The oral microbiome delivers important health benefits to the host.¹ Consequently, an important goal of oral care is to use strategies to manage the composition and metabolic activity of dental biofilms to maintain them at levels

compatible with oral health (ie, promote or maintain symbiosis while preventing dysbiosis). Sugar intake frequency and resulting acid production are the main risk factors for biofilm dysbiosis and caries. In our article, we modeled the effect of different frequencies of sugar intake per day and inhibition of acid production on dysbiosis.

Agents with an antibacterial or antimetabolism mode of action that become activated at low pH have the potential to modulate biofilm composition toward maintaining symbiosis, which is indicative of improved oral health. Such pH-intelligent designs have been explored as potential approaches to control the disease on the basis of pH-triggered antimicrobials or particles.^{22,23} Our modeling confirms that targeting acid production can be an effective stratagem to suppress biofilm dysbiosis, even under highly cariogenic pressures, though agents with a high degree of activity are necessary. For example, the well-known antimicrobial effect of fluoride is enhanced at lower pHs when fluoride can diffuse intracellularly as hydrogen fluoride.²⁴⁻²⁷ However, our model indicates that to be effective, these pH-dependent inhibitors would need to inhibit acid production at higher pH levels to be more effective against dysbiosis. This may explain why the antimicrobial role of fluoride is generally considered secondary to its physicochemical effect on the dynamics of mineral loss.⁴ The development of potential pH-dependent inhibitors into feasible anticaries alternatives may need to consider other factors such as agent substantivity (ie, the degree of retention of the inhibitor in the biofilm), which could be modulated by different strategies to be able to use previously known, but not effective inhibitors (eg, increasing the retention of fluoride in the dental biofilm).^{28,29}

Although our results confirm previous findings that, under normal conditions of saliva flow, subtle inhibitions of biofilm metabolism may have significant impacts on the biofilm ecological changes over time (the concept of controlling without killing⁶), they also offer a clear perspective on the limited power of inhibitors to overcome highly cariogenic challenges, such as that imposed by hyposalivation. Our data confirm the major impact of hyposalivation on driving dysbiosis,³ highlighting how much more drastic the inhibition of acid production would need to be in a dental biofilm exposed to conditions of low saliva flow ([Figures 2-4](#)). Under hyposalivation, inhibition of acid production could only shift the number of sugar intakes compatible with oral health by 1 through 2 exposures per day, and as hyposalivation causes dysbiosis at approximately one-half the frequency of sugar intake (as also shown in [Head et al](#)³) than normal flow rates, such inhibition is insufficient to change the behavior of a biofilm under hyposalivation closer to that of a biofilm under normal salivary flow ([Figure 2](#)). Only pH-dependent inhibitors working primarily above pH 5.5 ([Figure 3](#)) or inhibiting biofilm metabolism by more than 50% ([Figure 4](#)) would shift the safe sugar intake per day to a number closer to 4 under hyposalivation, and such agents are not available. Indeed, the data suggest that dietary control is a more fundamental strategy to prevent dysbiosis in patients with hyposalivation. Two or

fewer intakes of fermentable sugar per day are needed to maintain a symbiotic biofilm under hyposalivation; any more than this will drive dysbiosis. This frequency may be increased if inhibitors are present, but only minimally. As shown in the [Appendix](#) and the [sFigure](#) (available at the end of this article), including both forms of inhibition simultaneously does not alter these basic conclusions.

In addition, replacing fermentable sugars in the diet with nonmetabolizable sweeteners (eg, xylitol) would contribute to preventing dysbiosis and could be an alternative approach for these patients. These findings also emphasize the importance of testing saliva flow rates to identify at-risk patients and provide them with appropriate dietary advice at the earliest opportunity.

Individual-based biofilm models,¹⁰ such as the one we described, are well suited to predicting changes in composition during the maturation stage that initiates after the irreversible attachment of bacteria. Although specific details of the physical and chemical properties of saliva are not being modeled, previous work^{12,13} suggests the major effect of saliva on sugar clearance and, subsequently, biofilm pH, which is important for biofilm ecological shifts and caries, are being successfully modeled. Mathematical modeling avoids the ethical concerns of clinical studies and has been parameterized for bacterial species relevant to the human oral microbiome, specifically, obviating additional interpretation of animal models. Nonetheless, any model is necessary to simplify a more complex system, and restrictions on the availability of relevant data underpin model boundaries and limitations. Here, this means the microbial content of the biofilm is based on 2 functional groups,^{30,31} rather than an array of specific species that would vary between people. Additional functional groups, such as those that modulate acid production, could, in principle, be included with suitable parameterization once these data become available. However, the behavior of this model is consistent with what has been published in clinical studies.

Conclusions

The results confirm that the inhibition of acid production slows the rate of biofilm conversion from a symbiotic state to dysbiosis, which may reduce biofilm cariogenicity over time, and that hyposalivation has a profound effect on biofilm dysbiosis, reducing the number of sugar exposures per day that drive dysbiosis. The results suggest that even drastic inhibitions of biofilm metabolism may be insufficient to counteract the deleterious effects of hyposalivation and that, from a clinical standpoint, a restriction in fermentable sugar intake is paramount to control biofilm dysbiosis under hyposalivation.

Email d.head@leeds.ac.uk. Address correspondence to Dr Head.

Disclosure. None of the authors reported any disclosures.

This work was funded by the University of Leeds, United Kingdom, and the University of Michigan, Ann Arbor, MI.

ORCID Numbers. Deirde Devine: <https://orcid.org/0000-0002-8037-9254>; Livia M.A. Tenuta: <https://orcid.org/0000-0003-4626-4477>. For information regarding ORCID numbers, go to <http://orcid.org>.

References

- Kilian M, Chapple ILC, Hannig M, et al. The oral microbiome: an update for oral healthcare professionals. *Br Dent J.* 2016;221(10):657-666.
- Machiulskiene V, Campus G, Carvalho JC, et al. Terminology of dental caries and dental caries management: consensus report of a workshop organized by ORCA and cariology research group of IADR. *Caries Res.* 2020;54(1):7-14.
- Head D, Marsh PD, Devine DA, Tenuta LMA. In silico modeling of hyposalivation and biofilm dysbiosis in root caries. *J Dent Res.* 2021;100(9):977-982.
- ten Cate JM. Current concepts on the theories of the mechanism of action of fluoride. *Acta Odontol Scand.* 1999;57(6):325-329.
- Marsh PD, Head DA, Devine DA. Prospects of oral disease control in the future: an opinion. *J Oral Microbiol.* 2014;6:26176.
- Marsh PD, Head DA, Devine DA. Ecological approaches to oral biofilms: control without killing. *Caries Res.* 2015;49(suppl 1):46-54.
- Head D, A Devine D, Marsh PD. In silico modelling to differentiate the contribution of sugar frequency versus total amount in driving biofilm dysbiosis in dental caries. *Sci Rep.* 2017;7(1):17413.
- Bradshaw DJ, Marsh PD. Analysis of pH-driven disruption of oral microbial communities in vitro. *Caries Res.* 1998;32(6):456-462.
- Hamilton IR. Biochemical effects of fluoride on oral bacteria. *J Dent Res.* 1990;69 Spec No:660-667 [discussion: 682-683].
- Kreft JU, Picioreanu C, Wimpenny JWT, van Loosdrecht MCM. Individual-based modelling of biofilms. *Microbiology (Reading).* 2001;147(11):2897-2912.
- Head DA, Marsh PD, Devine DA. Non-lethal control of the cariogenic potential of an agent-based model for dental plaque. *PLoS One.* 2014;9(8):e105012.
- Dawes C. A mathematical model of salivary clearance of sugar from the oral cavity. *Caries Res.* 1983;17(4):321-334.
- Lagerlöf F, Dawes R, Dawes C. Salivary clearance of sugar and its effects on pH changes by *Streptococcus mitior* in an artificial mouth. *J Dent Res.* 1984;63(11):1266-1270.
- Ilie O, van Loosdrecht MCM, Picioreanu C. Mathematical modelling of tooth demineralisation and pH profiles in dental plaque. *J Theor Biol.* 2012;309:159-175.
- Ilie O, van Turnhout AG, van Loosdrecht MCM, Picioreanu C. Numerical modelling of tooth enamel subsurface lesion formation induced by dental plaque. *Caries Res.* 2014;48(1):73-89.
- Hase JC, Birkhed D. Salivary glucose clearance, dry mouth and pH changes in dental plaque in man. *Arch Oral Biol.* 1988;33(12):875-880.
- de Soet JJ, Nyvad B, Kilian M. Strain-related acid production by oral streptococci. *Caries Res.* 2000;34(6):486-490.
- Stralfors A. Studies of the microbiology of caries: the buffer capacity of the dental plaques. *J Dent Res.* 1948;27(5):587-592.
- Bradshaw DJ, Homer KA, Marsh PD, Beighton D. Metabolic cooperation in oral microbial communities during growth on mucin. *Microbiology (Reading).* 1994;140(12):3407-3412.
- Kinniment SL, Wimpenny JWT, Adams DJ, Marsh PD. Development of a steady-state oral microbial biofilm community using the constant-depth film fermenter. *Microbiology (Reading).* 1996;142(3):631-638.
- Stephan RM. Intra-oral hydrogen-ion concentrations associated with dental caries activity. *J Dent Res.* 1944;23(4):257-266.
- Naha PC, Liu Y, Hwang G, et al. Dextran-coated iron oxide nanoparticles as biomimetic catalysts for localized and pH-activated biofilm disruption. *ACS Nano.* 2019;13(5):4960-4971.
- Huang Y, Liu Y, Shah S, et al. Precision targeting of bacterial pathogen via bi-functional nanozyme activated by biofilm microenvironment. *Biomaterials.* 2021;268:120581.

24. Hamilton IR, Ellwood DC. Effects of fluoride on carbohydrate metabolism by washed cells of *Streptococcus mutans* grown at various pH values in a chemostat. *Infect Immun.* 1978;19(2):434-442.
25. Hamilton IR, Phipps PJ, Ellwood DC. Effect of growth rate and glucose concentration on the biochemical properties of *Streptococcus mutans* Ingbritt in continuous culture. *Infect Immun.* 1979;26(3):861-869.
26. Marsh PD, McDermid AS, Keevil CW, Ellwood DC. Effect of environmental conditions on the fluoride sensitivity of acid production by *S. sanguis* NCTC 7865. *J Dent Res.* 1985;64(2):85-89.
27. Germaine GR, Tellefson LM. Role of the cell membrane in pH-dependent fluoride inhibition of glucose uptake by *Streptococcus mutans*. *Antimicrob Agents Chemother.* 1986;29(1):58-61.
28. Vogel GL, Schumacher GE, Chow LC, Takagi S, Carey CM. Ca pre-rinse greatly increases plaque and plaque fluid F. *J Dent Res.* 2008;87(5):466-469.
29. Souza JGS, Tenuta LMA, Del Bel Cury AA, et al. Calcium pre-rinse before fluoride rinse reduces enamel demineralization: an in situ caries study. *Caries Res.* 2016;50(4):372-377.
30. Takahashi N. Oral microbiome metabolism: from “who are they?” to “what are they doing?” *J Dent Res.* 2015;94(12):1628-1637.
31. Espinoza JL, Harkins DM, Torralba M, et al. Supragingival plaque microbiome ecology and functional potential in the context of health and disease. *mBio.* 2018;9(6):e01631-18.

Appendix

Combined effect of pH-dependent and pH-independent inhibition

To ascertain the dominance of either of the 2 forms of inhibition, either pH-dependent or pH-independent, over the other, both were introduced simultaneously, and different combinations systematically varied. The results of these in silico assays are presented in the [sFigure](#), plotted on axes corresponding to each type of inhibition for the stated sugar intake frequencies. These frequencies were selected to correspond to biofilms that would be strongly or weakly dysbiotic in the absence of either form of inhibition. Both normal and hyposalivatory conditions were sampled, with the selected sugar frequencies for hyposalivation lower than those for normal conditions to give a comparable extent of dysbiosis without inhibition.

For sugar intake frequencies that placed the biofilm close to the symbiotic-dysbiotic transition but just into the dysbiotic regime, it was possible to promote symbiosis with less inhibition than biofilms deep into the dysbiotic regime. This is shown in the [sFigure](#), parts B and D, respectively, as evident from the narrow dysbiotic region near the origin of both of these plots. For higher sugar intake frequencies that

generated more strongly dysbiotic biofilms; however, much greater inhibition was required to restore symbiosis, as evident from the enlarged dysbiotic region in the [sFigure](#), parts A and C. As with the plots of inhibition against frequency discussed above, it was possible to discern the orientation of the symbiotic-dysbiotic boundary for these data, and the relative sensitivity to both forms in inhibition to be inferred.

When the pH-independent inhibition was less than 40%, the symbiotic-dysbiotic boundary was horizontal, as labeled IV in the [sFigure](#). In this region, the transition to dysbiosis occurred near the pH-dependent value $\text{pH}^{50\%}$ approximately 5.5, and was at most weakly independent of pH-independent inhibition. Thus, we can infer that pH-dependent inhibition dominates in this region of the parameter space. By contrast, for weak inhibitions in the approximate range $\text{pH}^{50\%}$ of 5 or less, the boundary becomes more vertically oriented, as labeled V in the [sFigure](#). As the transition to dysbiosis always occurs around a pH-independent inhibition of 60%, this suggests that pH-independent inhibition dominates over pH-dependent inhibition in this region of the diagram. However, the sparsity of data points makes it difficult to discern the true orientation of the boundary here definitively, and therefore, this conclusion remains tentative.

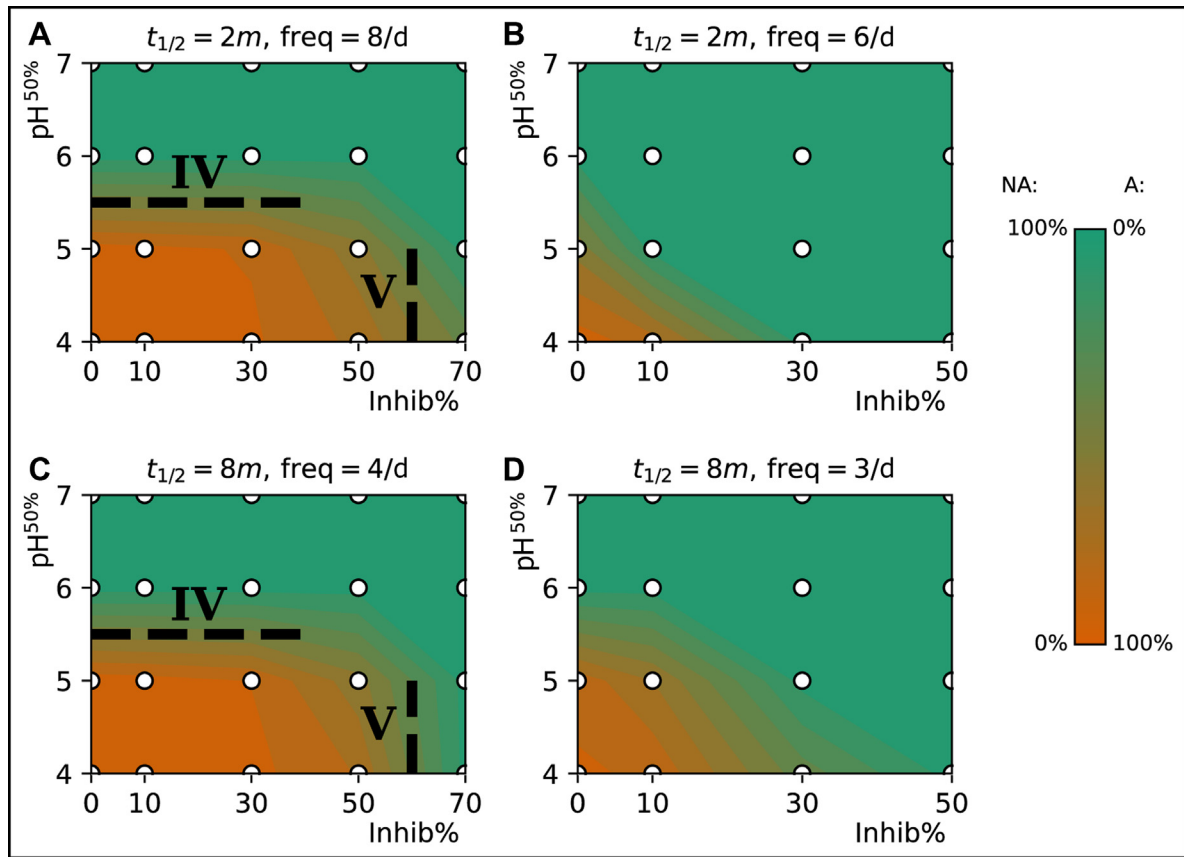


Figure Transition between symbiotic and dysbiotic biofilms under both pH-dependent and pH-independent (Inhib%) inhibition combined. The top row corresponds to normal salivary flow conditions (**A**, **B**), and the bottom row corresponds to hyposalivation (**B**, **D**). Conversely, the left column corresponds to sugar intake frequencies (freq) that would generate strongly dysbiotic biofilms in the absence of inhibition (**A**, **C**), and the right column to frequencies that would generate weak dysbiosis (**B**, **D**). The biofilm composition after 50 days is given by the calibration bar to the right, where A denotes aciduric particles, NA denotes nonaciduric particles, and white disks correspond to actual data points. The regions marked IV and V in **A** and **C** are discussed in the text.